



ELSEVIER

Journal of Chromatography A, 760 (1997) 3–16

JOURNAL OF
CHROMATOGRAPHY A

Influence of the heat of adsorption on elution band profiles in nonlinear liquid chromatography

Tong Yun^{a,b}, Peter Sajonz^{b,d}, Zouhir Bensetiti^{b,c}, Georges Guiochon^{b,c,*}

^aDepartment of Chemical Engineering, University of Tennessee, Knoxville, TN 37996-2200, USA

^bDivision of Chemical and Analytical Sciences, Oak Ridge National Laboratory, Oak Ridge, TN 37831, USA

^cDepartment of Chemistry, University of Tennessee, Knoxville, TN 37996-1600, USA

^dInstrumentelle Analytik, Umweltanalytik, Universität des Saarlandes, D-66123 Saarbrücken, Germany

Abstract

Fundamental investigations of band profiles in nonlinear liquid chromatography have always assumed isothermal conditions. This is correct in linear, analytical chromatography, in which case the solute concentrations are very small and the influence of the heat of adsorption on the band profiles can always be neglected. However, this is no longer exact in nonlinear chromatography because the concentrations of the feed components are usually high. If the heat of adsorption is large enough, the chromatographic system cannot be considered as isothermal. The differential heat and mass balance equations are then coupled. Experimental data acquired in a typical case illustrate the effect. These data fit well to a lumped kinetic model with slow heat transfer kinetics. Further calculations suggest that the influence of the heat of adsorption on actual separations is small and could be negligible in almost all cases.

Keywords: Band profiles; Heat of adsorption; Adsorption

1. Introduction

Theoretical studies of nonlinear liquid chromatography have always assumed isothermal conditions in the column [1]. This assumption is correct in linear chromatography because the solute concentrations are low: in principle, linear chromatography assumes infinite dilution; in practice analytical separations are performed at low concentrations. Accordingly, the effects of the heat of adsorption on the band profiles are very small and can be neglected. However, this assumption can no longer be entirely true in nonlinear chromatography. In this case, the concentrations of the feed components are usually high. If the heat of adsorption is high enough, the

chromatographic system cannot be considered as isothermal. The differential heat and the mass balance equations are therefore coupled. They must be solved together.

However, to the extent of our present knowledge, no instance has ever been reported in which the column eluent was significantly warmer during the elution of a large concentration band than when no feed component is leaving the column. A large number of investigations comparing experimental and calculated band profiles for single component and for binary mixtures, under a variety of experimental conditions has demonstrated excellent agreement between the two sets of data, provided that the equilibrium isotherms have been measured on the same column and properly modelled [1]. In all cases, thermal effects were neglected. This suggests

*Corresponding author.

that the thermal effects are either negligible or of minor importance under most sets of conditions encountered in common practice of preparative chromatography. In order to completely validate this assumption, however, it would be useful to investigate in a practical case the importance of the thermal effects due to the heat of adsorption (or more generally, to the heat associated with the passage of a compound from the mobile to the stationary phase).

The aim of this report is the description of the thermal effects observed during the elution of large size bands of phenol out of a preparative column packed with C_{18} bonded silica, the modelling of the temperature signals recorded at the column outlet and of the band profiles, and a discussion of the conditions required for the heat of adsorption to cause important changes in the separation between the components of a binary mixture.

2. Theory

To model the heat transfer in the chromatographic column, we assume that the system is adiabatic. In this case, the heat balance equation for the fluid phase is written as [2]:

$$\frac{\partial T_f}{\partial t} + u \frac{\partial T_f}{\partial z} + \frac{C_s}{C_f} \frac{(1-\varepsilon)}{\varepsilon} \frac{\partial T_s}{\partial t} + \frac{\Delta H}{C_f} \frac{\partial q}{\partial t} \frac{(1-\varepsilon)}{\varepsilon} = 0 \quad (1)$$

where C_f and C_s are the heat capacity of the fluid and solid phase, respectively; T_f and T_s are the temperatures of the fluid and solid phase, respectively; ε is the external porosity of the column packing (for the purpose of the heat balance, the solid adsorbent and the liquid in the pores must be lumped together), q is the concentration in the solid phase and ΔH is the enthalpy of adsorption.

The heat balance equation for the solid phase is:

$$\frac{\partial T_s}{\partial t} = h(T_f - T_s) - \frac{\Delta H}{C_s} \frac{\partial q}{\partial t} \quad (2)$$

where h is the heat transfer coefficient between the fluid and solid phase.

Note that the key parameters characterizing the intensity of the thermal signal are the ratios $\Delta H/C_f$, $\Delta H/C_s$ and C_s/C_f . This has two consequences. First,

the molar heat of adsorption alone is not a good indication of the magnitude of the effect. Secondly, it does not matter whether the adsorption enthalpy and the heat capacities are referred to the unit volume (as they should be, because balances are per unit volume) or to the unit mass, since this does not affect the dimension of these ratios.

The mass balance equation for the fluid phase is written as:

$$\frac{\partial C}{\partial t} + u \frac{\partial C}{\partial z} + \frac{(1-\varepsilon)}{\varepsilon} \frac{\partial q}{\partial t} = 0 \quad (3)$$

where C is the concentration in the fluid phase.

The mass transfer between the fluid phase and the solid phase is characterized by the solid-film linear driving force model:

$$\frac{\partial q}{\partial t} = k_f(q^* - q) \quad (4)$$

where k_f is the mass transfer coefficient between the fluid and the solid phase and q^* is the equilibrium concentration in the solid phase when the liquid phase concentration is C . q^* is calculated from the adsorption isotherm, which takes the form of the Langmuir model, with q_s the saturation capacity and b the energy term, given by:

$$q^* = \frac{q_s b C}{(1 + b C)} \quad (5)$$

b is calculated from the following equation, where b_0 is a numerical constant:

$$b = b_0 \exp\left(\frac{-\Delta H}{RT}\right) \quad (6)$$

The boundary and initial conditions of the problem are those corresponding to the injection of a narrow plug of solution of the compound at a concentration C_0 during a time t_p , at a temperature T_0 , in a column free of sample:

$$C(0,t) = C_0 \quad 0 < t \leq t_p \quad (7a)$$

$$C(0,t) = 0 \quad t_p < t \quad (7b)$$

$$C(z,0) = 0 \quad 0 < z \quad (7c)$$

$$T_f(z,0) = T_s(z,0) = T_0 \quad 0 < z \quad (7d)$$

The solution of this model of chromatography, with a finite rate of mass transfer kinetics and a finite (slow) rate of heat transfer between fluid and solid phase, depends on the mass transfer and heat transfer coefficients. The other parameters, i.e. the heat capacities for the fluid and solid phase, were taken from the literature [3]. b_0 and ΔH were estimated from adsorption isotherm data measured at different temperatures. h was estimated by best fitting to the experimental results. The best value so obtained is later compared to the value given by conventional correlations.

Using a finite difference program, numerical solutions of the system of equations discussed above [Eqs. (1)–(7d)] were calculated for the conditions corresponding to the experiments performed and described later. In these calculations, k_f was determined from the column efficiency measured just after completion of the packing, C_s was estimated from the heat capacity of sand and C_f from the heat capacities of water and methanol [3].

Finally, we note that Rhee et al. [4] have studied a similar problem, using the equilibrium theory. They have shown that, during the saturation of an initially clean bed (i.e. a bed equilibrated with the pure mobile phase) with a feed, a positive thermal zone forms and migrates before the concentration (or mass) zone. Thus, a positive temperature peak must elute in front of the concentration band. Because desorption is endothermic and takes place along the rear, diffuse concentration profile of the band, a negative temperature band follows. Thus, in the same time as the concentration band, a thermal band is eluted. This band includes a positive and a negative temperature peak. The areas of these two peaks are equal since, after elution of the band, the column returns to equilibrium (no feed left in the column, isothermal column at initial temperature).

3. Experimental

3.1. Isotherm measurement

The isotherm data were measured using a Hewlett–Packard 1090 liquid chromatograph (Hewlett–Packard, Palo Alto, CA, USA), equipped with a UV detector, a computer data acquisition system and a

multi-port solvent delivery system. A circulating water-bath was used to control the temperature of the analytical column during the entire investigation. The solvent and the sample were preheated to the same temperature set up for the column, in order to minimize the temperature gradients in the whole instrument. The experimental conditions are as follows:

3.1.1. Column

A 15×0.46 cm column was packed in the laboratory with Zorbax C₁₈ bonded silica (10 μm, 100 Å) from BTR Separations (Wilmington, DE, USA).

3.1.2. Solvent

For all chromatographic runs, the mobile phase was methanol–water (40:60, v/v). HPLC grade water and methanol (Baxter, Muskegon, MI, USA) were used, without further purification. The flow-rate of the mobile phase was always 1.00 ml/min.

3.1.3. Chemicals

Phenol (Fisher Scientific, Fairlawn, NJ, USA) was used without further purification. Phenol was chosen because of its high solubility in the mobile phase (more than 100 g/l at 25°C) and its relatively low retention factor on C₁₈ silica (cf. Table 1), so the sample band is eluted shortly after its introduction into the column, which avoids serious heat losses through the column wall during its migration.

3.1.4. Procedures

The adsorption isotherms were obtained by frontal analysis. The column was submerged in the circulating water-bath to control the column temperature within ±0.1°C, at each of the five temperatures at which the amounts adsorbed were measured: 288.2, 298.2, 308.2, 318.2 and 328.2 K. Pure mobile phase and a 80.4 mg/ml solution of phenol in the mobile phase were placed in two flasks of the solvent delivery system. The injection of a series of concentration steps from 0 to 80.4 mg/ml was programmed on the chromatograph data station, using the gradient generating facility, and the corresponding breakthrough curves were recorded. Before acquiring data at a new temperature, the system was run for at least one hour to ensure that it was

Table 1
Isotherm parameters^a used in this work

	Temperature (K)				
	288.2	298.2	308.2	318.2	328.2
a^a	3.627	2.988	2.389	2.046	1.706
b^a	0.04343	0.03810	0.03086	0.02900	0.02555
q_s^a	83.51	78.44	77.42	70.54	66.79

^a b and q_s , parameters of the Langmuir isotherm [Eq. (5)] for phenol under the experimental conditions used. The parameter $a = bq_s$ is the initial slope of the isotherm.

thermally stable. Previous experiments have shown flow-rates to be constant within 1–2 $\mu\text{l}/\text{min}$ over several hours [5].

The best-fit Langmuir isotherm parameters were calculated by using a Marquardt method available from SAS [6]. The values of the parameters, a , b and q_s , determined at the different temperatures are listed in Table 1. The heat of adsorption was derived from the slope of the plot of $\log b$ vs. $1/T$.

3.2. Measurement of the heat signal

3.2.1. Thermocouple

The thermocouple (model TJ72-CPSS-116U-12, from Omega Engineering, Stamford, CT, USA) is a copper wire housed in a 304 stainless steel sheath, 1/16 in. O.D. and 12 in. long (1 in. = 2.54 cm). The signal was converted (TAC 386+C A/D convertor from Omega) and transferred to the data acquisition system (NEC computer and Waters, Milford, MA, USA, Maxima software). The thermocouple was calibrated and its output found to be linear in the temperature range from -200 to 360°C with a response which fitted to the function $T(\text{K}) = 992.4V(\text{mV}) + 268.1$, with a relative standard error of 0.48%. The design and construction of the thermocouple are suitable for operation under rugged conditions, e.g., inside the packing of an axial compression column.

3.2.2. Dynamic axial compression column

The heat signal measurements were performed on a Prochrom (Champigneulle, France) LC50 system, consisting of a 50 cm \times 50 mm I.D. stainless steel column and a dynamic compression system. A stainless piston is moved inside the column by a hydraulic jack. This system keeps constant the axial

compression stress applied by the piston to the bottom of the column packing [7,8]. The thermocouple was inserted inside the packing through a hole in a home-made top flange and secured in place with ferrule and fitting. The tip of the thermocouple is located approximately 5 cm below the exit frit, inside the packing, and 1.0 cm from the column axis. The total length of packing was approximately 13.8 cm. Thus the concentration profile is recorded at the end of a 13.8 cm long column, the temperature profile at the end of a 8.8 cm long column. This difference was taken into account when calculating the corresponding profiles.

3.2.3. Solvent delivery system

A Kiloprep 100 HPLC pumping system (Biotage, Charlottesville, VA, USA) was used in this work. The pump is designed to deliver solvents at a flow-rate up to 500 ml/min, and a maximum pressure of 138 bar. The system includes also an injection valve and a 10 ml injection loop.

3.2.4. Chemicals and packing material

The column was packed with Zorbax C_{18} bonded silica packing material coming from the same bottle as the packing used for the isotherm measurements. The mobile phase was prepared by mixing distilled water, filtered on a 1.2 μm membrane, with 99.9% methanol, purchased from Mallinckrodt (St. Louis, MO, USA) and used without further purification.

3.3. Experimental procedure

The axial compression column was packed under normal conditions, by filling it with a slurry of packing material in pure isopropanol, placing the end frit and the top flange, fastening them and applying

the compression stress [7,8]. Then, isopropanol was replaced by the methanol–water (40:60, v/v) solution, used as the mobile phase, and the column was flushed for 10 h before further experiments. The flow-rate was 51 ml/min, the column efficiency was measured under linear conditions, using, as the sample, a dilute solution of phenol in the mobile phase. The column void volume was derived from the retention volume of uracil, obtained during the efficiency measurements.

After the column had been prepared, it was wrapped with glass wool fibre (Aldrich, Milwaukee, WI, USA), to prevent radial heat losses, and the top flange was replaced by the laboratory-made flange with the thermocouple attached to it. However, this operation could not be performed without causing a severe reduction in the apparent column efficiency. Either the column bed was too strongly disturbed around the thermocouple when it was inserted inside the packing, causing significant local compression stress and strain, or the flow distributor in the laboratory-made flange was not quite as good as the manufacturer's and plug flow could not be maintained in the last part of the column, causing radial heterogeneity in the flow-rate distribution at the column outlet. As it happened, the part of the bed disturbed is above the tip of the thermocouple and the distributor perturbed is on the exit side. As a consequence, the zone moves through an efficient bed until it flows by the tip of the thermocouple and the temperature profile recorded corresponds to the migration in the initial column bed, the same as before placing the temperature sensor. The temperature profile observed should correspond to the one calculated using the parameters measured on this initial column. These temperature profiles should also correspond to the band profiles recorded on the initial column or calculated with its parameters, allowing for a short reduction in column length.

Finally, the column was flushed with mobile phase from a constant temperature tank for a couple of hours, until it reached hydrodynamical steady-state and thermal equilibrium, as determined by monitoring the column temperature with the thermocouple. Then samples of concentrated phenol solutions were injected and the output of the thermocouple recorded with the data acquisition system. Later, the data files were uploaded to the computer of the

University of Tennessee Computer Center for further processing.

4. Results and discussion

Fig. 1 illustrates the isotherm data acquired between 15 and 45°C (symbols) and the best Langmuir model (lines) of these data. The best values of the parameters, obtained by nonlinear regression, are collected in Table 1. Fig. 2 shows a comparison between the calculated profiles of the elution bands and the chromatograms recorded during experiments performed with the same analytical column. The sample size (20.1 mg) corresponds to a loading factor of 24.5% at 15°C, 26.1% at 25°C and 29.0% at 45°C (the loading factor is the sample amount reported to the column saturation capacity). The 3 chromatograms were recorded at different temperatures, 15, 25 and 45°C. The agreement is very good in all three cases, demonstrating the self-consistency of the isotherm and kinetics determination, and of the column behavior. The slight differences between the tails of the calculated and experimental profiles suggest a slight underestimation of the amount adsorbed at equilibrium with the mobile phase at low concentrations, probably because breakthrough profiles were not recorded for low enough values of the concentration.

Fig. 3 shows a plot of the logarithm of the coefficient b of the Langmuir isotherm vs. $1/T$. In this narrow temperature range, the small difference between the heat capacities of phenol in the solution and in the adsorbed phase has a negligible effect on the curvature of the plot, which can be considered as a straight line. The data points (symbols) fit well to a straight line. The adsorption enthalpy derived from the slope of this line is -2.04 kcal/mol (8.52 kJ/mol), a rather typical value in reversed-phase liquid chromatography.

Fig. 4a–c show the results obtained in three successive experiments. The figures give the plots of the temperature of the eluent recorded vs. time (symbols), upon injection of large amounts of phenol, corresponding to values of the loading factor of 20.1, 20.1 and 40.1%, respectively (these values are based on a column length equal to the distance between the column inlet frit and the tip of the

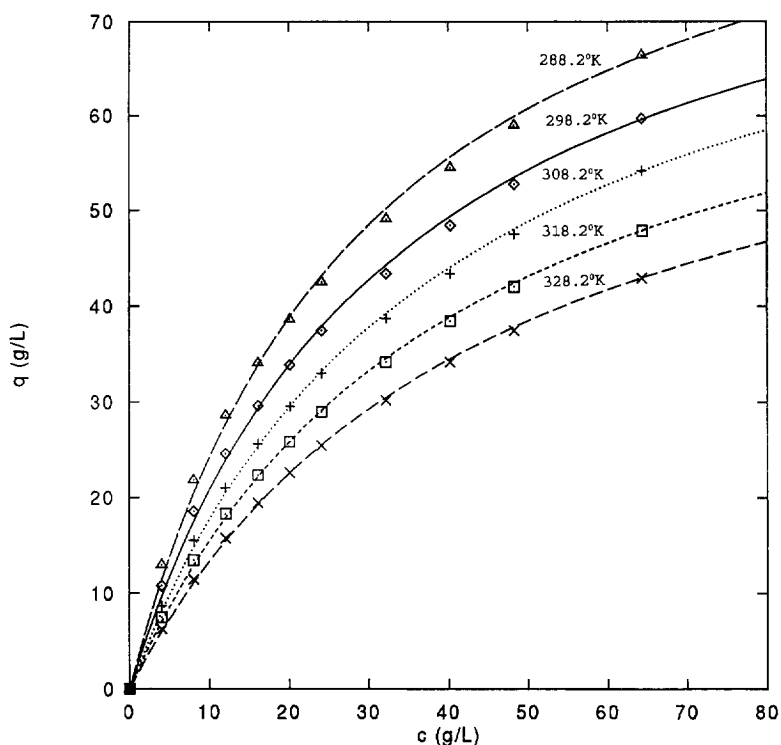


Fig. 1. Isotherm data. Plots of the amount adsorbed at equilibrium versus the mobile phase concentration. Experimental conditions in text.

temperature sensor, approximately 12 cm). The dashed lines in these figures are the temperature profiles calculated as explained above in Section 2. The heat transfer coefficient, h , has been determined so as to give the smallest distance between the calculated and experimental profiles. There is an excellent agreement between these two sets of thermal profiles, the only significant difference being in the tails of the bands and reflecting the same underestimation of the isotherm curvature at low concentrations, as already seen in Fig. 2. We note that the temperature signal has a narrow positive peak of +1.5 K followed by a broad, tailing negative peak of -0.8 K for a loading factor of 20.1%. These values are relatively small and seem insufficient to cause any major change to the calculated band profiles if they were neglected. Note, finally, the excellent reproducibility of the experimental results (cf. Fig. 4a–b).

The value obtained for the rate constant of the heat transfer kinetics is low at 0.3 s^{-1} . It is approximately fifteen times smaller than the rate constant of the

kinetic mass transfer between the mobile and the stationary phase, 4.36 s^{-1} . Both values, however, are in reasonably good agreement with independent estimates of these two parameters, which can be done using correlations found in the literature.

A recent correlation was developed by Ohashi et al. [9]

$$\text{Sh} = 2.0 + 1.58\text{Sc}^{1/3} \text{Re}^{0.4} \quad (8)$$

for $0.001 < \text{Re} < 5.8$

where Sh is the Sherwood number ($\text{Sh} = d_p k_f / D_L$), Sc is the Schmidt number ($\text{Sc} = \mu / \rho D_L$) and Re is the Reynolds number ($\text{Re} = u d_p \rho / \mu$). The mobile phase is methanol–water (40:60, v/v). Its density is 0.9442 g/ml [3], its viscosity at 20°C is 1.6 cP [3] and the average particle size is $10 \text{ }\mu\text{m}$. The Brownian diffusion coefficient is not available for ternary systems such as the one studied. It was estimated to be $5.41 \cdot 10^{-6} \text{ cm}^2/\text{s}$ (from the correlation published in ref. [11]). Accordingly, the Reynolds and Schmidt numbers are 0.00397 and 3390, respectively. The

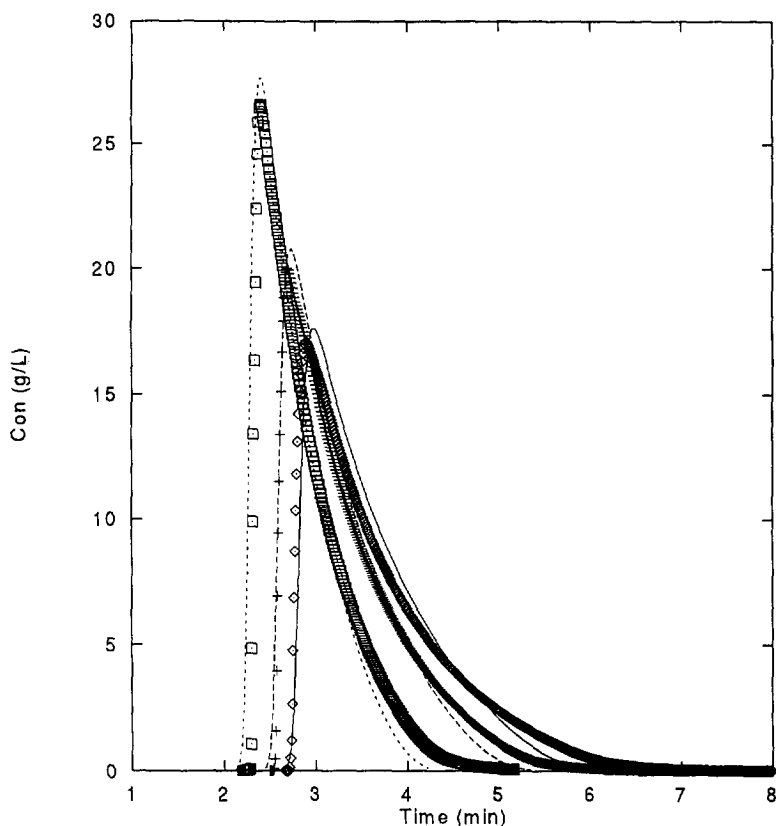


Fig. 2. Comparison between experimental (symbols) and calculated (lines) band profiles. Column dimension: 15×0.4 cm; flow-rate = 1.0 ml/min; phase ratio = 0.651; injection volume = 0.25 ml; injection concentration = 80.385 g/l; isotherm data, refer to Table 1. \diamond : Experimental data at 288.2 K; solid line: calculated data at 288.2 K; +: experimental data at 298.2 K, long dash line: calculated data at 298.2 K, \square : experimental data at 318.2 K, short dash line: simulated data at 318.2 K.

correlation gives $Sh = 4.60$ and $k_f = 23 \text{ s}^{-1}$. This value is in poor agreement with the experimental result ($k_f = 4.36 \text{ s}^{-1}$).

There are far fewer correlations in the literature regarding heat transfer than mass transfer kinetics. Most of them are for gas–solid systems. According to Kunii and Levenspiel [10], we may estimate h by using the following correlation

$$Nu = 2.0 + 1.8Pr^{1/3} Re^{1/2} \quad (9)$$

where Nu is the Nusselt number ($Nu = hd_p/k_i$) and Pr is the Prandtl number ($Pr = \mu C_p/k_i$). In the definitions of these numbers, h is the heat transfer coefficient, C_p the heat capacity of the mobile phase and k_i the thermal conductivity of the mobile phase. For methanol–water (40:60, v/v), the thermal con-

ductivity is $0.00145 \text{ cal s}^{-1} \text{ cm}^{-1} \text{ K}^{-1}$, and the heat capacity is $860 \text{ cal l}^{-1} \text{ K}^{-1}$ (1 cal = 4.184 J). This gives a Prandtl number equal to 0.05, hence a Nusselt number of 2.24. The corresponding value of h is 3.7 s^{-1} . This value is in poor agreement with the experimental result (0.30 s^{-1}). The disagreement between our experimental results and the value given by the correlation is important. It is not too surprising, however, because of the important differences between the experimental conditions encountered in liquid chromatography and those under which the correlations have been established. The main differences are the extremely small size of the particles used (although we are dealing with dimensionless analysis, we must remember that extrapolation is a dangerous business) and the chemically bonded layer of octadecyl groups at the silica surface, which could

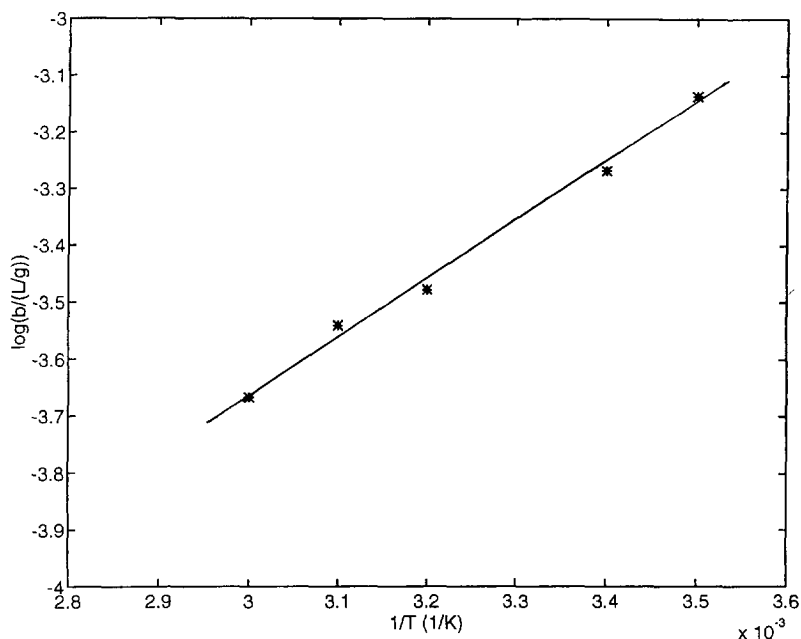


Fig. 3. Temperature dependence of the parameter b of the Langmuir isotherm. * – Experimental data; line – the result from linear regression; it is determined from this figure: $\Delta H = 2040.03$ cal/mol; $b_0 = 0.00137$ l/g.

affect, markedly, the liquid–solid rate of heat transfer.

Fig. 5 shows the calculated thermal signals and the elution band profiles calculated as solutions of the model discussed above, in the case of phenol under the experimental conditions selected for this work (Fig. 4a–c). The thermal signals include the temperature profiles in the stationary phase (T_s) and in the mobile phase (T_r). These last two curves differ essentially by the small temperature peak observed in the T_s profile at the time of elution of the shock layer of the overloaded elution band. We notice also a time lag between T_r and T_s . Because of its design, however, the experiment performed allows the measurement of T_r only. The maximum temperature is eluted before the band begins to exit from the column and the minimum temperature coelutes with the inflection point on the rear diffuse boundary of the concentration profile.

Fig. 6 compares the elution band profiles calculated with three different values of the heat of adsorption, 0, -2.05 and -8.2 kcal/mol, all corresponding to a compound of molecular mass 94 (like, e.g., phenol). The first value is the one generally

assumed in most fundamental studies: it is the value consistent with the implicit assumption made when the effect of the heat of adsorption on the band profiles is neglected. The second value is the one obtained in the case of phenol in reversed-phase liquid chromatography. The last value corresponds to a hypothetical compound which would be strongly adsorbed through a mechanism which involves the formation of two hydrogen bonds or, at least, of very strong polar interactions (such as observed, e.g., in chiral selective retention mechanisms). The differences between the first two elution bands are very small, too small to be demonstrated experimentally with any accuracy. By contrast, the third band is broader and shorter than the other two. The relative increase in the band width and the relative decrease in the band height compared to the width and height of an isothermal band are sufficiently large to be measured, should they take place in a real case. However, a heat of adsorption of -8.2 kcal/mol or 87 cal/g is rather large and situations of this type are bound to be unusual or even exceptional in liquid chromatography.

Under our experimental conditions, the concen-

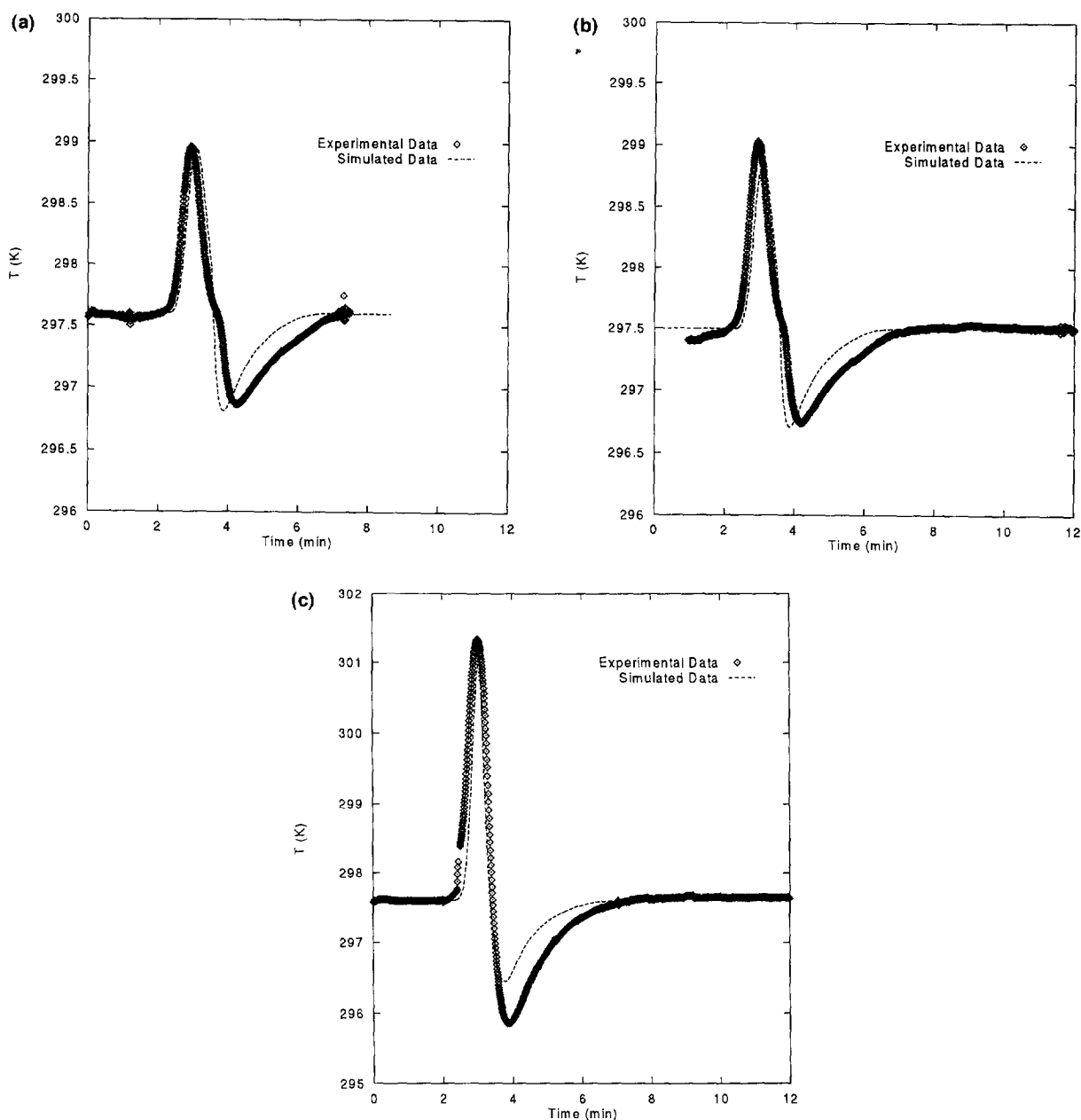


Fig. 4. Comparison between experimental (symbols) and calculated (lines) profiles of temperature of the eluent. (a) Column dimension: 8.8×5.0 cm; flow-rate = 51.0 ml/min; phase ratio = 0.553; injection volume = 10.0 ml; injection concentration = 95.511 g/l; $\Delta H = 2040.03$ cal/mol; $C_i = 860$ cal l^{-1} K^{-1} ; $C_s = 512$ cal l^{-1} K^{-1} ; $k_i = 4.36$ s $^{-1}$; $h = 0.30$ s $^{-1}$; baseline temperature = 297.6 K. (b) Same as Fig. 4a except the baseline temperature = 297.5 K. (c) Injection volume = 20.0 ml; others same as Fig. 4a.

tration profile of the elution band is not strongly affected by the adsorption heat, as illustrated in Fig. 6. Because of the importance of the heat of ad-

sorption required to observe a significant effect, we are of the opinion that the influence of the heat of adsorption on the band profiles will be negligible in

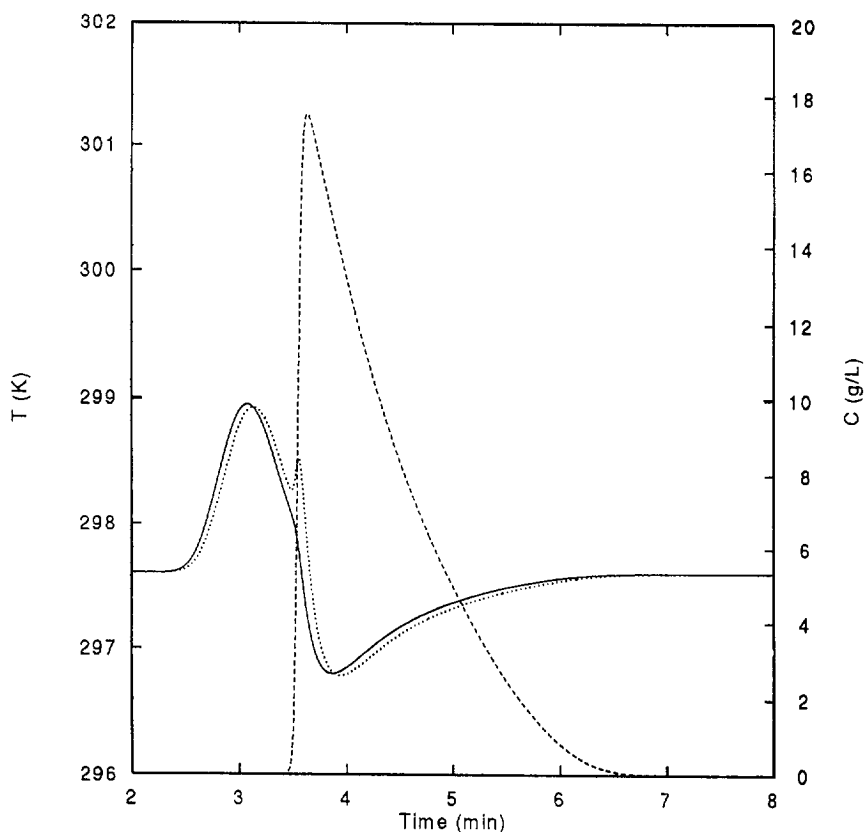


Fig. 5. Thermal and concentration signals calculated at the exit of the column. $\Delta H = 2040$ cal/mol; the other conditions are the same as in Fig. 4a. Solid line = T_r , dotted line = T_s , dashed line = concentration. (b) Same as in Fig. 4a.

almost all cases of any practical interest in the preparative applications of chromatography, at least in reversed-phase liquid chromatography. Heat of adsorption is prone to be larger in the separation of enantiomers on chiral selective phases than in most other separations. The chiral recognition mechanism involves the formation of complexes between the enantiomers and the stationary phase. These complexes are strongly bonded, usually by hydrogen bonding and heats of adsorption in the 7 to 10 kcal/mol range. However, the molecular mass of such compounds is often of the order of 200 to 300, resulting in values in the range of 20 to 50 cal/g only. Note that the important parameters in Eqs. (1) and (2) are the heat of adsorption reported to the heat capacity of the liquid and solid phase, all parameters are reported to the unit mass of adsorbate or phase, not to the mole.

For example, in the separation of N-benzoyl-D and L-alanine ($M_r = 209$) on immobilized bovine serum albumin, the isosteric heat of adsorption has been determined to be -6.51 and -5.01 kcal/mol, respectively, for the two enantiomers on the enantio-selective sites and -2.77 kcal/mol on the nonselective sites [12]. These heats of adsorption are 3, 24 and 13 cal/g, respectively (vs. 22 cal/g for phenol in this work). The intensity of the thermal effect corresponding to these values will be relatively small. The adsorption enthalpy of the *R* and *S* enantiomers of propranolol ($M_r = 295$) on immobilized cellobiohydrolase (a protein) was determined to be -3.66 and $+3.36$ kcal/mol, respectively, for the enantio-selective retention mechanism [13]. These values are rather small. Furthermore, the saturation capacities of enantio-selective phases are usually low, so small samples are injected and, although the

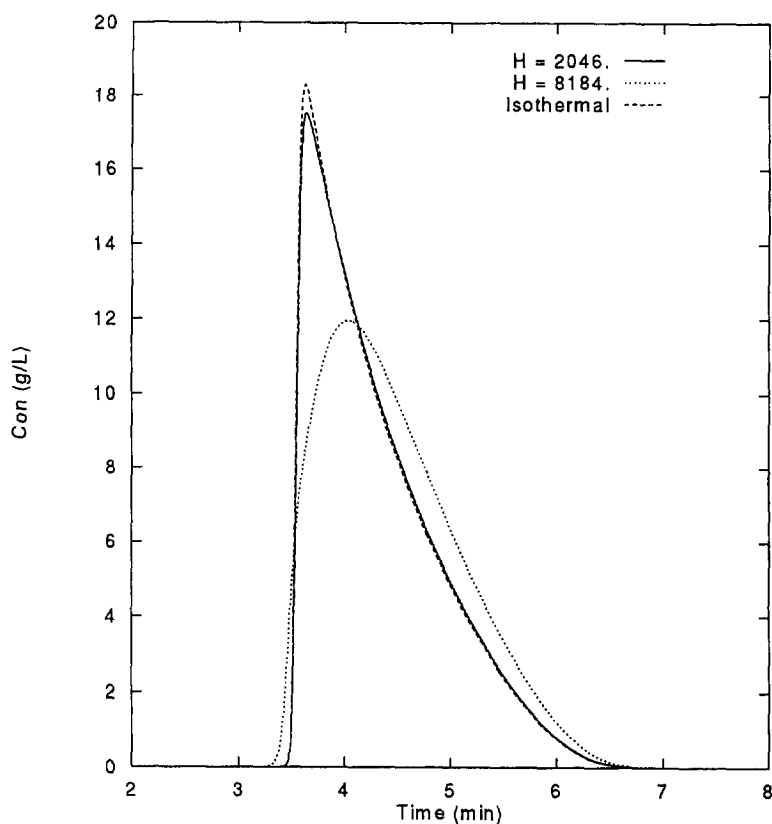


Fig. 6. Comparison of band profiles of compounds differing only by their heat of adsorption. Solid line: $\Delta H=204$ cal/mol; dotted line: $\Delta H=8160$ cal/mol; dash line: $\Delta H=0$ cal/mol, isothermal condition. $C_r=740$ cal l^{-1} K^{-1} , $k_r=3.0$ s $^{-1}$. Other parameters are the same as Fig. 4a.

column is highly overloaded, the elution bands have low concentrations and this can result only in small heat effects. Higher values of the heat of adsorption are possible in normal-phase chromatography, because silica is able to give strong hydrogen bonding or acid–base interactions with polar compounds. With high values of the adsorption heat, however, the retention would be extremely high. Only the use of a strong solvent could reduce it. Unfortunately, in the process, the heat of adsorption would also be reduced, to more reasonable values. Only under some extreme and exceptional set of conditions, resulting in both a high heat of adsorption and a high entropy of adsorption, will a fast enough elution be compatible with high adsorption energies. Then, as shown in Fig. 6, the elution profiles can be strongly affected by the heat effect.

Be as it may, it is useful at this stage, for the sake

of completeness, to calculate the elution profile of a binary mixture and determine what is the range of heat of adsorption within which the separation begins to be significantly altered by the interaction of the concentration and thermal profiles. Fig. 7a–c show the results of such calculations. In each of these figures, the main figure shows three total concentration profiles, while the inset shows the two individual band profiles calculated by the same program in the only case of the strongest thermal effect; these profiles could not be shown in the main figure, for the sake of clarity. The cutpoints for the production of components 1 and 2 at 99 and 98% purity from a 1:1 mixture and the recovery yields achieved are reported in Tables 2–4 for the experimental conditions selected in Fig. 7a–c. These are not the optimum conditions for maximum production rate but these results illustrate quantitatively

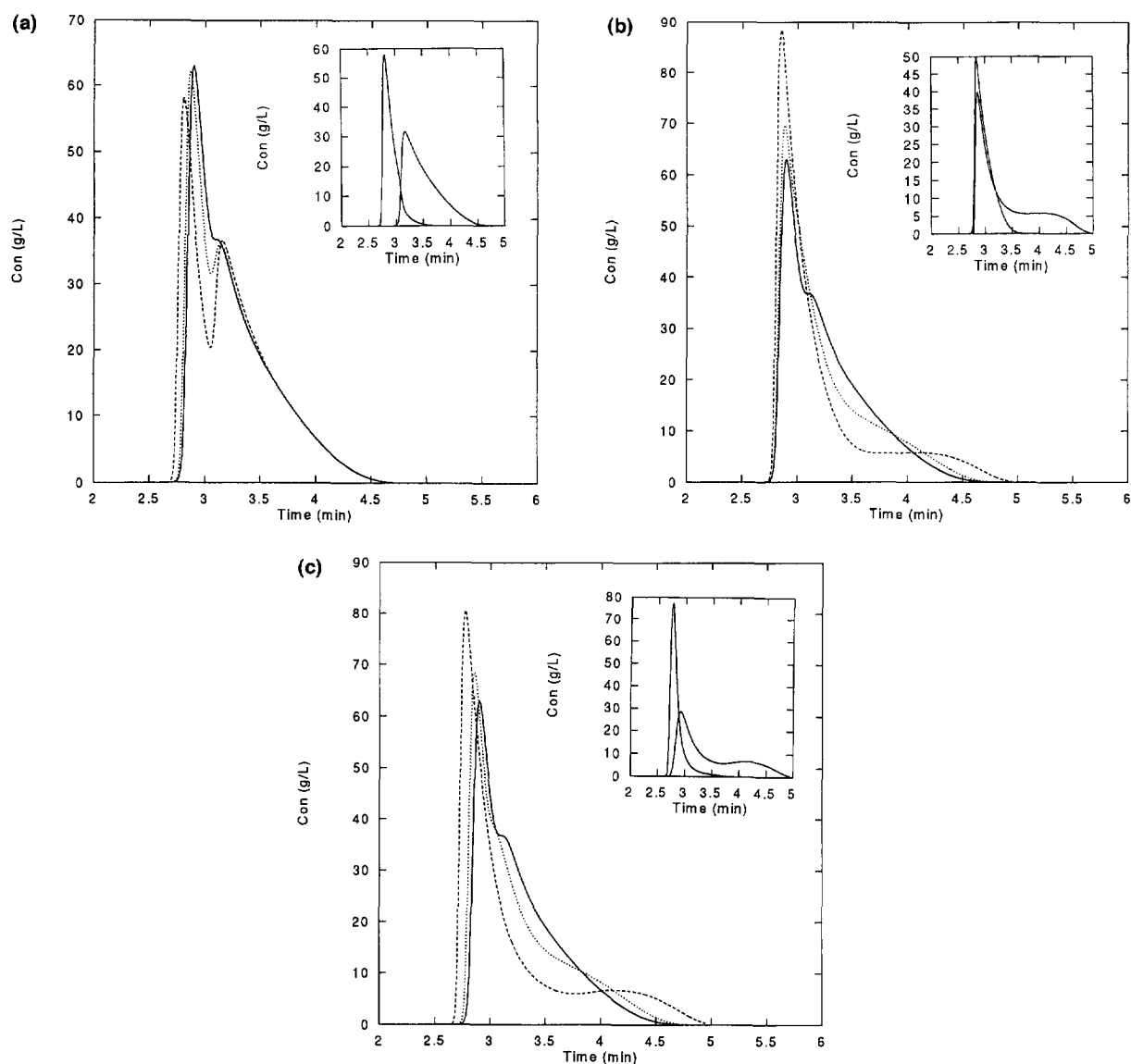


Fig. 7. Calculated chromatograms for binary mixtures under adiabatic conditions. Experimental conditions: (a) The heat of adsorption of the second component is small (1 kcal/mol), that of the first one is: 1 kcal/mol; --- 7 kcal/mol; — 15 kcal/mol. (b) The heat of adsorption of the first component is small (1 kcal/mol), that of the second one is: 1 kcal/mol; --- 7 kcal/mol; — 15 kcal/mol. (c) The heat of adsorption of both components is: 1 kcal/mol; --- 7 kcal/mol; — 15 kcal/mol.

the conclusions drawn from the visual examination of the band profiles.

In Fig. 7a, the adsorption heat of the second component remains constant, equal to 1 kcal/mol, while that of the first component increases from 1 (4.17) (practically no thermal effect, see Fig. 6), to 7

and 15 kcal/mol. Both compounds have a molecular mass of 94. The situation is somewhat similar to that observed for some enantiomeric separations (see above), at least for the second chromatogram. It is interesting to observe that, in this case, the separation is actually markedly improved by the thermal effect.

Table 2
Position of the cut-points for 99 and 98% purity and recovery yields^a

		Component 1 (Less retained)	Component 2 (More retained)
$\Delta H_1 = 1.0$ kcal/mol	99% purity	179.17 s/65.27%	200.76 s/59.21%
$\Delta H_2 = 1.0$ kcal/mol	98% purity	181.09 s/74.41%	196.39 s/68.87%
$\Delta H_1 = 7.0$ kcal/mol	99% purity	181.37 s/77.86%	197.02 s/68.07%
$\Delta H_2 = 1.0$ kcal/mol	98% purity	182.85 s/82.79%	202.036 s/57.03%
$\Delta H_1 = 15.0$ kcal/mol	99% purity	184.01 s/87.68%	208.12 s/45.40%
$\Delta H_2 = 1.0$ kcal/mol	98% purity	184.99 s/89.41%	200.85 s/60.02%

^a Data for Fig. 7a, arbitrary compounds with properties as described in the caption of Fig. 7.

Table 3
Positions of the cut-points for 99 and 98% purity and recovery yields^a

		Component 1 (Less retained)	Component 2 (More retained)
$\Delta H_1 = 1.0$ kcal/mol	99% purity	179.17 s/65.27%	200.76 s/59.21%
$\Delta H_2 = 1.0$ kcal/mol	98% purity	181.09 s/74.41%	196.39 s/68.87%
$\Delta H_1 = 1.0$ kcal/mol	99% purity	173.47 s/31.21%	204.00 s/49.22%
$\Delta H_2 = 7.0$ kcal/mol	98% purity	174.96 s/42.86%	200.17 s/54.77%
$\Delta H_1 = 1.0$ kcal/mol	99% purity	165.57 s/0.15%	210.17 s/34.30%
$\Delta H_2 = 15.0$ kcal/mol	98% purity	166.17 s/0.33%	207.14 s/36.07%

^a Data for Fig. 7b, arbitrary compounds with properties as described in the caption of Fig. 7.

The recovery yields at both degrees of purity increase with increasing heat of adsorption of the first component (Table 2). This phenomenon is easily explained by the acceleration of the migration of the first component band, which migrates in the wake of the thermal wave generated by its adsorption (see the position of the positive temperature peak in front of the concentration band in Figs. 4 and 5).

Fig. 7b shows the converse case, when the heat of adsorption of the first component remains constant

and equal to 1 kcal/mol, while that of the second increases from 1 to 7 and to 15 kcal/mol. The degree of separation achieved between bands decreases with increasing thermal effect, because the higher the heat of adsorption of the second component the faster its band migrates. The recovery yield decreases with increasing heat of adsorption of the second component (Table 3). Finally, Fig. 7c shows the more conventional case when the heat of adsorption of both components are equal to 1, 7 and 15 kcal/mol.

Table 4
Positions of the cut-points for 99 and 98% purity and recovery yields^a

		Component 1 (Less retained)	Component 2 (More retained)
$\Delta H_1 = 1.0$ kcal/mol	99% purity	179.17 s/65.27%	200.76 s/59.21%
$\Delta H_2 = 1.0$ kcal/mol	98% purity	181.09 s/74.41%	196.39 s/68.87%
$\Delta H_1 = 7.0$ kcal/mol	99% purity	174.75 s/53.32%	204.23 s/51.38%
$\Delta H_2 = 7.0$ kcal/mol	98% purity	176.62 s/64.56%	199.01 s/59.33%
$\Delta H_1 = 15.0$ kcal/mol	99% purity	165.43 s/20.55%	218.00 s/35.50%
$\Delta H_2 = 5.0$ kcal/mol	98% purity	166.76 s/32.90%	210.29 s/39.39%

^a Data for Fig. 7c, arbitrary compounds with properties as described in the caption of Fig. 7.

In this case also, the degree of separation decreases with increasing heat of adsorption and the recovery yields decrease (Table 4).

5. Conclusion

In principle, the heat of adsorption has an effect on the concentration profiles observed in chromatography. Chromatograms are different depending on whether the column is operated under adiabatic or isothermal conditions. However, while it is possible to ensure nearly adiabatic conditions, it is not possible to keep isothermal any column used for preparative applications. The stationary phases used in chromatography are good thermal insulators. A classical model combining the heat and mass balance equations with kinetic equations for mass and heat transfers allows the calculation of elution and thermal profiles, which are in excellent agreement with experimental results. The kinetic of heat transfer between the mobile and the solid phase is more than an order of magnitude slower than the mass transfer kinetic. The values of the heat and mass transfer coefficients derived from experimental data are not in good agreement with values derived from conventional correlations, probably because typical chromatographic conditions are far remote from conventional range of experimental conditions investigated in chemical engineering. Particularly at variance are the size of the particles and the chemistry of the surface (the C_{18} bonded layer could slow down considerably the heat transfer kinetics).

However, in practice, the influence of this heat effect on the band profiles and on the separations performed by liquid chromatography is negligible in at least a very large majority of cases. This confirms the implicit conclusions of most practitioners and theoreticians of chromatography, that excellent results are obtained while assuming that the columns are operated under isothermal conditions.

One of the important results of this work is to show that, under conventional chromatographic conditions, the heat transfer coefficient is more than one order of magnitude smaller than the mass transfer

coefficient (15 times). Our experimental results are certainly not compatible with a rate constant of heat transfer comparable to or larger than the mass transfer rate constant.

Acknowledgments

This work was supported in part by grant CHE-92-01663 from the National Science Foundation and by the cooperative agreement between the University of Tennessee and the Oak Ridge National Laboratory. We acknowledge the continuous support of our computational efforts by the University of Tennessee Computing Center. TY thanks George Frazier for the stimulative graduate course received on this topic in the Department of Chemical Engineering of The University of Tennessee.

References

- [1] G. Guiochon, S.G. Shirazi and A.M. Katti, *Fundamentals of Preparative and Nonlinear Chromatography*, Academic Press, Boston, MA, 1994.
- [2] D.M. Ruthven, *Principles of Adsorption and Adsorption Processes*, Wiley, New York, 1984.
- [3] R.C. Weast (Editor), *Handbook of Chemistry and Physics*, 72nd ed., CRC Press, Boca Raton, FL, 1991.
- [4] H.K. Rhee, E.D. Heerd and N.R. Amundson, *Chem. Eng. J.*, 1 (1970) 279.
- [5] M.Z. El Fallah and G. Guiochon, *Anal. Chem.*, 63 (1991) 859.
- [6] *SAS Manual*, SAS Institute, Cary, NC, 1992.
- [7] M. Sarker and G. Guiochon, *J. Chromatogr. A*, 702 (1995) 27.
- [8] M. Sarker and G. Guiochon, *J. Chromatogr. A*, 709 (1995) 227.
- [9] H. Ohashi, T. Sugawara, K. Kikuchi and H. Konno, *J. Chem. Eng. Jpn.*, 14 (1981) 433.
- [10] D. Kunii and O. Levenspiel, *Fluidization Engineering*, 2nd ed., Butterworths-Heinemann, London, 1991.
- [11] Perry (Editor), *Handbook of Chemical Engineering*, 6th ed., McGraw-Hill, New York, 1984.
- [12] S.C. Jacobson, S. Golshan-Shirazi and G. Guiochon, *J. Chromatogr.*, 522 (1990) 23.
- [13] T. Fornstedt, P. Sajonz, G. Zhong, Z. Benseititi and G. Guiochon, *Anal. Chem.*, in press.